Iraqi National Journal of Earth Science

www.earth.mosuljournals.com

Mineralogy and Geochemistry of Coastal Sabkha Deposits Along Yakhtul Coast, Red Sea, Yemen

Saeed Omar Wasel [1], Badir N. Albadran [2*]

[1]*Marine Geology Department, Faculty of Marine Science and Environment, University of Hodeidah, Yemen.*

[2] *Department of Petroleum Engineering, University of Almaaqal, Basrah, Iraq.*

Article information

Received: 19- Apr -2023

Revised: 25- Sep -2023

Accepted: 16- Oct -2023

Available online: 01- Jan – 2024

Keywords:
Mineralogy
Geochemistry
Yakhtul Sabkha
Red Sea Coast
Yemen

Correspondence:
Name: Badir N. Albadran

Email:
Wasel9@hoduniv.net.ye.

ABSTRACT

The surface sediments of the coastal sabkha region in the southern part of the Red Sea region in Yemen are studied mineralogically and geochemically to determine their provenance. Using the X-ray diffraction technique, the evaporite minerals are identified in the sabkha area represented by gypsum, halite, and anhydrite. Carbonate minerals are represented by calcite, aragonite, and dolomite, whereas quartz and feldspars represent non-evaporite minerals. Smectite, kaolinite, chlorite, illite, and palygorskite are the predominant clay minerals, mainly of detrital origin. Mineralogical assemblages present in the sediments largely control the abundance and distribution of total carbonates, organic matter content, and the major and trace elements. Geochemically, the factor controlling the carbonate content of the studied sediments includes the calcareous material of biogenic and terrigenous components. However, the carbonate content of the marine sediments varies from 8.96 to 41.70%, with an average of 18.55%. The organic matter content of the sediments is between 0.36 and 0.87%. The distribution of major elements Fe, Ca, Mg, Na, K, and Mn and trace elements Cu, Zn, Cd, Ni, Pb, and Co in the sabkha sediments of the study area vary considerably and could be attributed to the sediment sources.

DOI: 10.33899/earth.2023.139633.1066,

معدنية وجيوكيميائية رواسب السبخة الساحلية على طول ساحل يختل ، البحر الأحمر ، اليمن

سعيد عمر واصل [1] ، بدر نعمة البدران [2*]

[1] *قسم الجيولوجيا البحرية، كلية علوم البحار والبيئة، جامعة الحديدة، اليمن.*

[2] *قسم عندسة النفط ، كلية الهندسة، جامعة المعقل، البصرة ، العراق.*

معلومات الارشفة

تاريخ الاستلام: 19- ابريل -2023

تاريخ المراجعة: 25- سبتمبر -2023

تاريخ القبول: 16- اكتوبر -2023

تاريخ النشر الالكتروني: 01- يناير -2024

الكلمات المفتاحية:

علم المعادن

الجيوكيمياء

سبخة يختل

ساحل البحر الأحمر

اليمن

المراسلة:

الاسم: بدر نعمة البدر

Email: Wasel9@hoduniv.net.ye

الملخص

تمت دراسة الرواسب السطحية لمنطقة السبخة الساحلية في الجزء الجنوبي من منطقة البحر الأحمر في اليمن من الناحية المعدنية و الجيوكيميائية لتحديد مصدرها. باستخدام تقنية حيود الأشعة السينية، تم تحديد معادن المتبخرات في منطقة السبخة وهي الجبس والهاليت والأنهيدرايت. شخصت معادن الكربونات كالكالسيت والأراغونيت والدولوميت، بينما يمثل الكوارتز والفلسبار معادن غير متبخرات. السميكتايت، الكاؤلينيت، الكلوريت، الإيليت، والباليغورسكيت هي معادن الطين السائدة، خاصة من أصل فتاتي. تتحكم التجمعات المعدنية الموجودة في الرواسب إلى حد كبير في وفرة وتوزيع إجمالي الكربونات، ومحتوى المادة العضوية، والعناصر الرئيسة والنزرة. من الناحية الجيوكيميائية، يشمل العامل الذي يتحكم في محتوى الكربونات في الرواسب المدروسة المواد الجيرية للمكونات الحيوية والفتاتية. ومع ذلك، يتراوح محتوى الكربونات في الرواسب البحرية من 8.96 إلى 41.70٪ بمتوسط 18.55٪. يتراوح محتوى المادة العضوية في الرواسب بين 0.36 و 0.87٪. اختلف توزيع العناصر الرئيسية Fe، Ca، Mg، Na، K، Mn والعناصر النزرة Cu، Zn، Cd، Ni، Pb، Co في رواسب السبخة في منطقة الدراسة بشكل كبير ويمكن أن تعزى إلى مصادر الرواسب.

DOI: 10.33899/earth.2023.139633.1066,

Introduction

Sabkha deposits are one of the Arabic expressions to describe the recent sediments with high salt content. The sabkha is of two types, either a coastal sabkha or an inland sabkha within the continent. Coastal sabkhas are supratidal flat surfaces shaped by the depositional overlaps of marine sediments, and the associated evaporites are derived from seawater (Kinsman, 1969). The active sabkha is underlain through porous sediments that supply groundwater as well as marine water to preserve place with the water lost through evaporation at the surface (Purser, 1973).

The coastal sabkhas are of interest to many researchers than the inland sabkhas. On the basis of morphological and hydrodynamic characteristics, Gavish (1980) classified coastal sabkhas into two models; supratidal and sea marginal brine pans.

The recent coastal sabkha deposits are considered an outstanding phenomenon along the Red Sea coast, however, they remained extraordinarily untouched and there is an obvious lack of knowledge on mineralogy and geochemistry in these coastal environments.

Therefore, the purpose of this research is to investigate the mineralogical and geochemical characteristics of the sediments that were deposited in this coastal sabkha.

Study area

Yakhtul Sabkha is situated 160 km south of Hodeidah City, on the eastern coast of the Red Sea of Yemen. This sabkha is parallel to the line of the coast (Fig. 1). Its length is 9.5 km and its maximum width is 2 km.

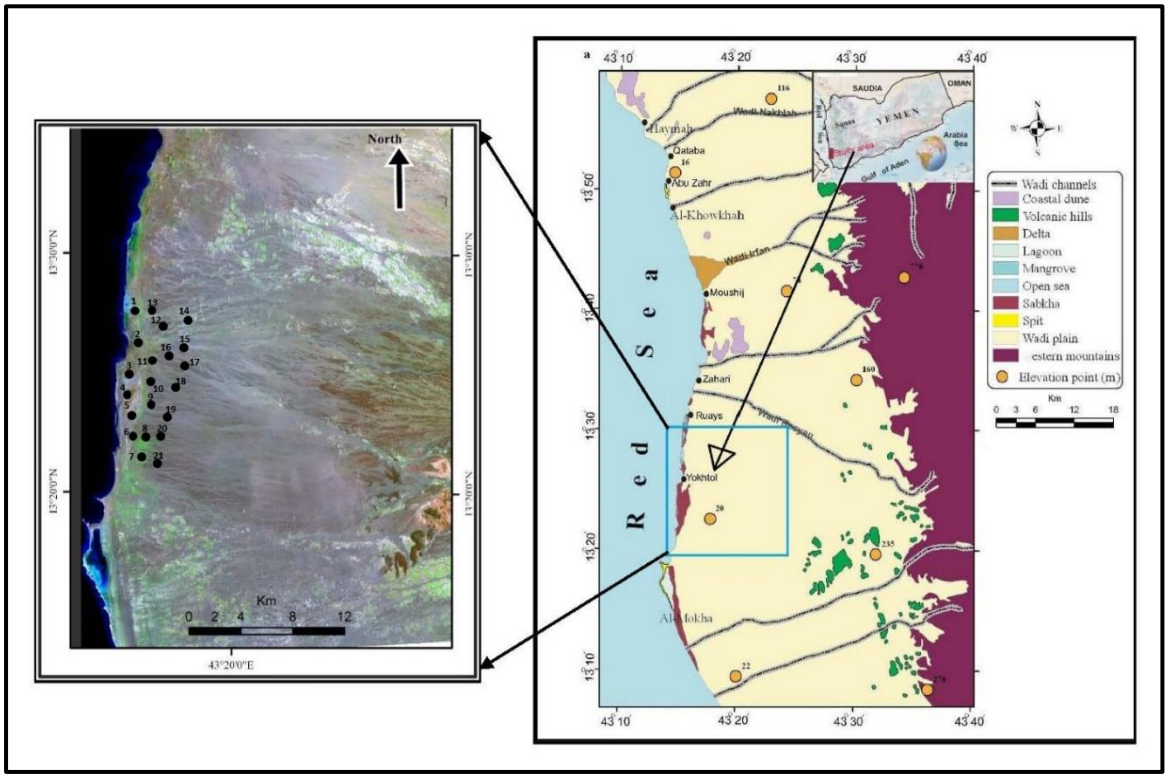

Fig.1. Location map of the sediment samples in the studied Yakhtul sabkha and the geomorphic features on the Red Sea coast.

The direction of the sabkha surface slope is towards the coast, and this sabkha is separated by a wide beach ridge of coastal sand dunes (Fig. 2).

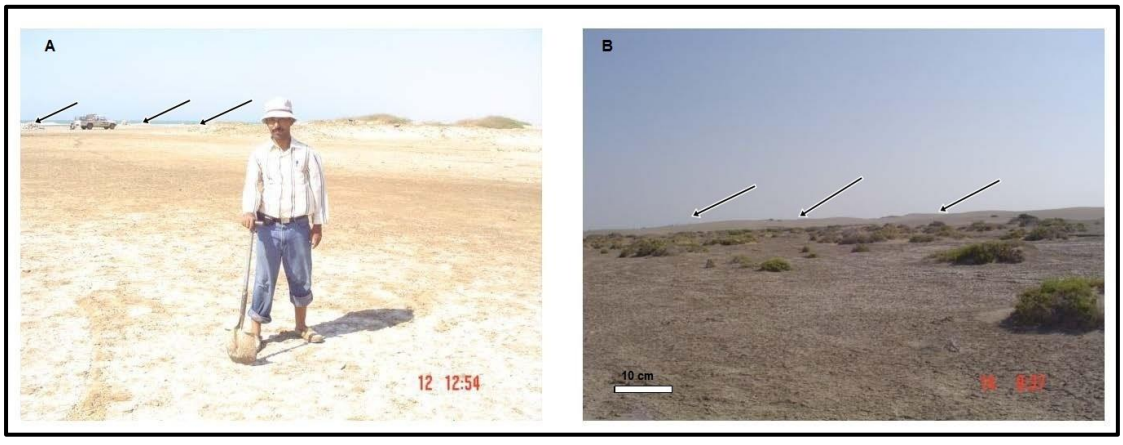

Fig. 2. The boundary between Sabkha and the Sea. (A) Barren sabkha covered by evaporite crust. (B) Vegetated sabkha around the barren sabkha.

The flat plain of the study area consists of muddy sand texture, which covers low areas, valleys, and tidal flats. The percentage of gravel is about 1%, sand is about 86%, and mud is about 13% (Wasel and Al-Zubieri, 2023). The areas surrounding the study area, are covered with Pleistocene and Recent sediments, mainly made up of eolian sand and gravels that were derived from the eastern Red Sea mountainous escarpment made up of basic (basalt, andesite, andesitic pyroclastics), acidic (dacite and rhyolite) volcanic rocks, and granitic rocks, particularly those of Tertiary age (El-Younsy et al., 2017). Several drainage channels (wadis) flow westward into the Red Sea and occasionally disappear in Tihama. The wadis are tremendously dry most of the year. They activate temporarily; therefore, representing important channels for sediments and fresh water to the Red Sea coast through incidental major floods (Fig. 1). These valleys are responsible for transporting the muddy sand sediments to the coastal regions.

Climate

The climate of the area in the Tihama basin is very dry, where the average annual rainfall is of 100-200 mm/year, and the humidity is about 60 percent. There are no permanent surface streams discharging into the Red Sea, even though flash floods are a widespread feature following torrential rains. In some places, the seepage of groundwater is due to the wetting of the coast. This seepage of the groundwater happens close to the surface and is lost through evaporation. Generally, the climatic conditions of the Red Sea area are low rainfall and high temperatures.

The studied area is characterized by a hot and dry climate, with about 50 mm of rain fairly well distributed throughout the year. The prevailing wind, in general, is almost NNW and SSE (Edward and Head, 1987). The salinity of the water in Al-Khowkhah is like other coastal areas along the Red Sea, ranging between 37.3‰ and 38.73‰. The corresponding surface water temperatures are between 32.10° C and 34.40° C (Rushdi et al., 1994). Both the temperature and salinity values of the surface seawater could indicate the mixing process of the water in the coastal area.

Material and Methods

Twenty-one sabkha samples are collected from the surface sediments. Most of the collected samples are from the barren sabkha whose number is 14, while the selected samples of vegetable sabkha are 7. The sampling in the study area, starts from 20 meters apart from the coastline up to 500 meters. The sediments are rather solid because they are covered with a thin layer of evaporites. Grain size analysis of the sediments show that they are mostly muddy sand. X-ray diffraction (XRD) technique is applied to bulk minerals and to each clay mineral. Twenty-one dried samples of muddy sand texture are powdered for X-ray diffraction analysis. Seven samples are separated using a pipette method for clay fractions analyses (Galehouse, 1971). Three steps of X-ray diffraction are carried out for oriented samples; untreated, glycolated, and heated (550°C for 3 h), using a Philips X-ray diffractometer at Assiut University with Cu Kα radiation, 45 kV, and 35 mA. Mineral identification is based on the detection of the characteristic diffraction peaks using tables of key lines listed by Chao (1969) and Chen (1977). The area under the peak of the biggest intensity for each mineral present has been measured and the relative percentage of each

mineral has been calculated according to Carver (1971) and Tucker (1988). This method of calculation is doubled, once on the diffractogram for clay mineral assemblage alone, and again for the diffractogram of the powdered total minerals assemblage alone.

Ten grams from ten dried samples are selected and crushed by agate mortar for the geochemical analysis; total carbonates, organic matter, and some major and trace elements.

The amount of total carbonate is determined by treating the samples with 1 N HCl acid. The remaining insoluble residue is determined to calculate the carbonate percentage. Organic matter is determined by sequential weight loss at 550 °C (Dean, 1974).

Metal constituents are measured by Atomic Absorption Spectrophotometer using the extraction method mentioned in Loring and Rantala (1992). Extractive analysis differs from total digestion analysis, as the former represents the withdrawal of elements that adhere to the mineral crystals only, while digestion analysis, is a complete crushing of all minerals by a strong mixing of hydrofluoric and nitric acids. Therefore, the sum of the elements represents the minerals themselves, as well as the elements that have adhered to the crystals.

Field Observations

The sabkhas of the study area could be classified into barren and vegetated sabkhas. The barren sabkha covers most of the central part of the topographic depression of the sabkha. This sabkha is wet and composed of sand, halite crust, and mud, deposited on the supratidal flat (Fig. 2A). The vegetated sabkha are covered by salt-tolerant halophytes that can live in hypersaline conditions (Figs. 2B and 3E, F).

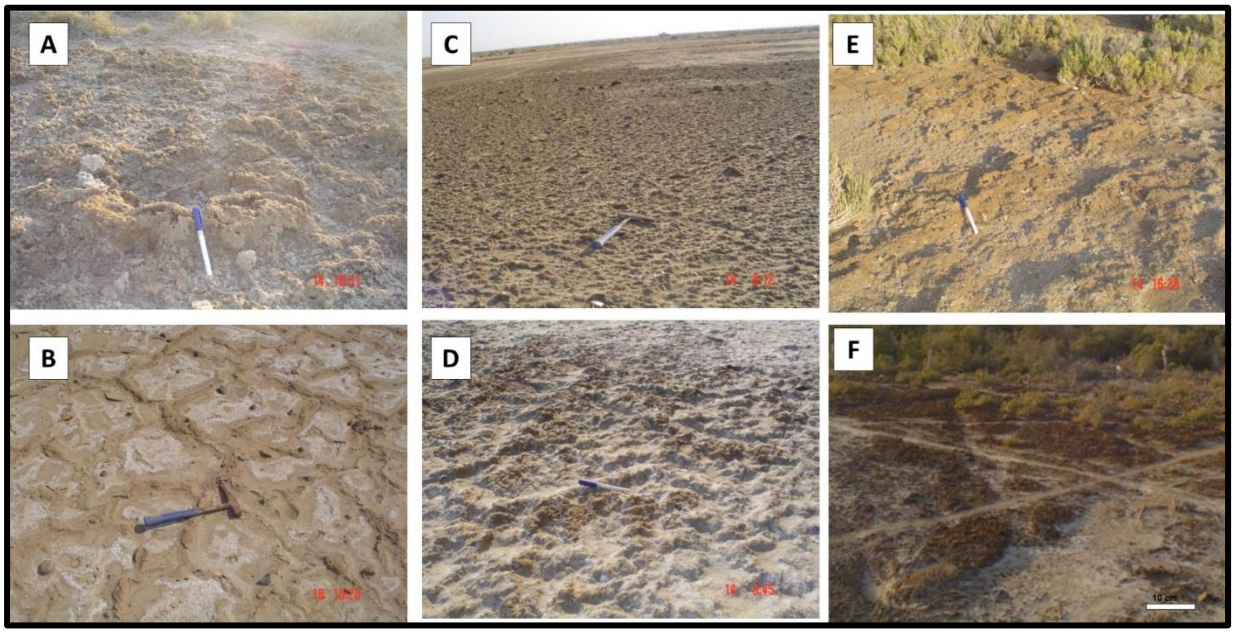

Fig. 3. Surface features of sabkha and sedimentary structures in the study area. A) Development of tepee structure due to the displacive growth of evaporate minerals. B) Polygonal patterned surface showing the orthogonal type of polygonal tepee structures. C) Wet zone along the sabkha margin with the growth of small petee structures. D) Well developed petee structure due to the combination of the physical forces of crystallization and the biogenic growth effect. E) Suaeda pruinosa in sandy sabkha facies. F) Aeluropus massauensis in sandy and muddy sabkha facies.

Field investigation has shown that the surface of the sabkha exhibits an elevated zone, covered with a tepee structure (Figs. 3A and 3B). This zone is completely dry during summer and wet during winter. The heights of the tepee structures vary from immature types to mature types. During winter, the tepee structures like mega ripples, since the wind is strong and a higher level of water-table leads to the wetting of sediments. The immature tepees are small puffy halite structures near the saline ponds, whereas, mature types are big, and their bedding is cracked into slabs, which show overthrusting. The tepee structures may be resulted either from the instability between the underlying wet layers, due to evaporative pumping, or the overlying rigid one resulted from the evaporation. The rupture of crests of tepee structures in this zone could be increased with increasing the intensity of crystals resulting in surface expansion (Kendall and Warren, 1987; Attia, 2013; Aref et al., 2014). It is possible that the tepee would have been more developed if the salinity and temperature were higher as the case of Khor Al-Zubair in southern Iraq (Albadran and Al-Kaaby, 2021).

Some parts of the sabkha are covered by microbial mats (Fig. 3C and D), which are produced by cyanobacteria in hypersaline environments (Cohen et al., 1977; Gerdes and Krumbein 1987; Attia, 2013; Aref et al., 2014, Manaa and Aref, 2022). The intense horizontal and vertical growth of cyanobacteria can alter the surface sediment properties, where these cyanobacteria lead to produce structures called microbially induced sedimentary structures (MISS). The growing microbial mats and the precipitated salt crystals (gypsum, halite) could be responsible for the development of the petees structures (Noffke, 2010 and Lakhdar et al., 2021). These structures are bio-sedimentary surface structures completely different from abiogenic tepee structure. Both structures appear in the study area (Fig. 3).

Results

The results of X-ray diffraction of the bulk samples are mentioned in (Table 1) and the diffractograms are given in figure (4).

Table 1: Relative percentages of bulk minerals determined in sabkha deposits.

Sample No.	Quartz	Orthoclase	Plagioclase	Calcite	Aragonite	Dolomite	Gypsum	Anhydrite	Halite
1	12.45	1.60	8.77	7.60	4.68	13.20	38.70	0.60	12.40
2	25.40	1.20	4.35	4.11	2.10	6.28	32.14	6.52	17.90
3	10.40	0.00	1.30	8.20	0.00	11.20	48.60	0.00	20.30
4	15.93	6.71	10.30	1.90	1.40	0.00	35.60	7.76	20.40
5	20.30	0.00	3.93	9.77	6.20	0.00	40.30	2.30	17.20
6	17.95	8.36	10.00	14.30	4.90	0.00	28.30	0.00	16.20
7	15.70	0.00	6.20	12.40	11.20	2.70	38.40	0.00	13.40
8	17.35	6.20	8.60	12.94	10.80	5.40	24.80	1.31	12.60
9	24.60	6.08	11.41	5.32	14.07	0.80	26.42	0.00	11.30
10	10.80	1.60	4.80	1.50	0.00	15.20	41.25	1.70	23.15
11	15.93	6.71	11.74	2.30	0.00	0.00	31.80	7.20	24.32
12	16.72	0.00	9.29	8.05	4.95	15.48	37.46	0.00	8.05
13	31.06	0.00	4.90	4.63	0.00	7.08	24.80	7.36	20.16
14	1.39	0.00	0.00	0.00	0.00	22.69	50.93	0.00	25.00
15	16.17	6.81	11.91	0.00	0.00	0.00	20.64	7.87	36.60
16	19.64	16.58	10.97	26.02	5.36	0.00	3.83	0.00	17.60
17	15.64	0.00	8.14	38.44	34.85	2.93	0.00	0.00	0.00
18	17.61	7.61	16.42	13.13	14.63	8.81	7.16	2.69	11.94
19	16.89	4.43	8.81	12.90	8.54	8.14	20.69	2.56	17.05
20	23.50	14.20	0.00	18.20	1.70	0.00	24.30	1.70	16.40
21	21.10	12.40	6.20	10.80	0.00	2.40	25.20	6.30	15.60
Max.	31.06	16.58	16.42	38.44	34.85	22.69	50.93	7.87	36.60
Min.	1.39	0.00	0.00	0.00	0.00	0.00	0.00	0.00	0.00
Aver.	17.45	4.79	7.53	10.12	5.97	5.82	28.63	2.66	17.03

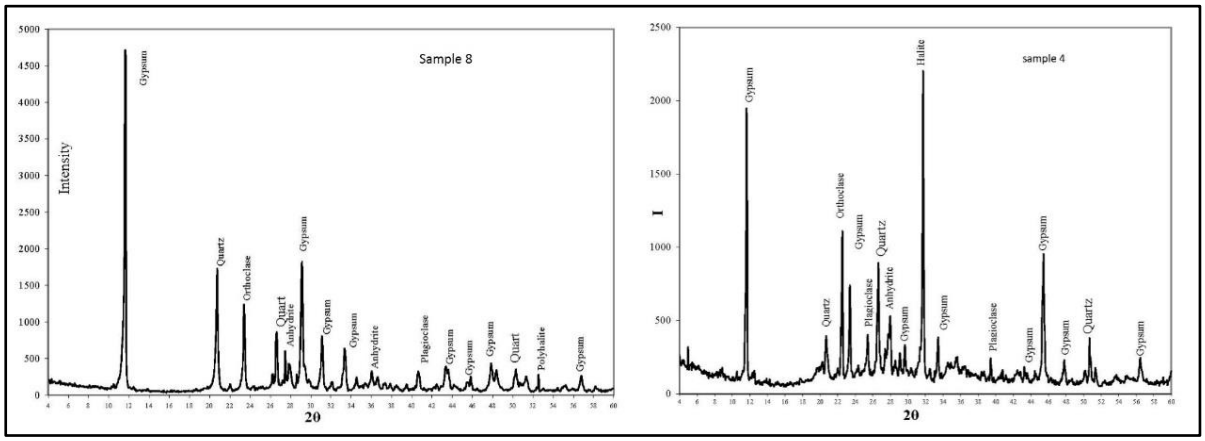

Fig. 4. X-ray diffractograms of representative bulk minerals from the studied sabkha deposits.

The obtained percentages of bulk minerals are represented graphically in figure (5). Gypsum, halite, and anhydrite represent the evaporite minerals. Gypsum is the predominant recorded sulfate mineral ranging from 0.0% to 50.93% with an average of 28.63%. Halite is the second evaporite mineral recorded in the investigated area with percentages varying from 0.0% to 36.59% with an average of 17.03%. Anhydrite content differs from 0.0% to 7.87% with an average of 2.66%. The carbonate minerals are represented mainly by calcite, with minor amounts of aragonite and dolomite (Fig. 5). Calcite value varies from 0.0% and 38.44% with an average of 10.12%. Aragonite is recorded in some samples with values ranging from 0.0 to 34.85% and an average of 5.97%. Dolomite value varies from 0.0% to 22.69% with an average of 5.82%. Detrital minerals are represented by quartz and feldspars (Fig. 5). Quartz occurs in all samples in amounts ranging between 1.39% and 31.06% with an average of 17.45%. Feldspar minerals are mainly represented by plagioclase and K-feldspar. Plagioclase recorded in the investigated sabkha sediments with a percentage varies from 0.0% to 16.42% with an average of 7.53%, while K-feldspar varies between 0.0% and 16.58% with an average of 4.78%.

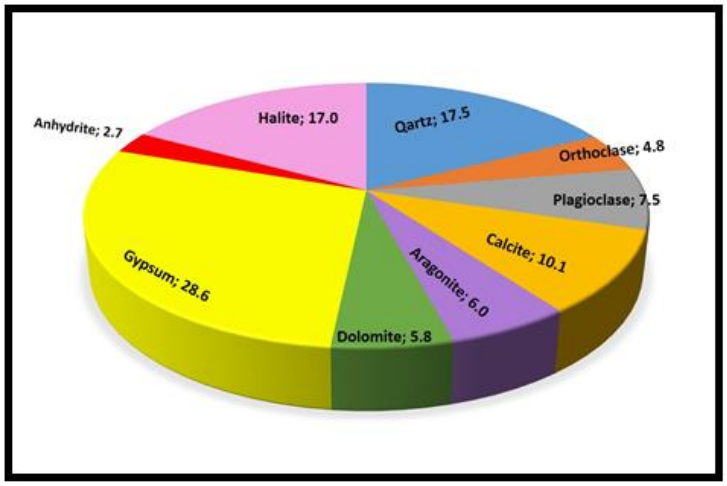

Fig. 5. Bulk minerals average of the sabkha deposits

The content of smectite (Table 2 and Fig. 6) in the sediments of sabkha is between 31.83 and 47.08% with a mean of 37.44% in the sabkha deposits. The amount of chlorite ranges between 12.13 and 29.18%. The amount of kaolinite in the sabkha sediments is from 15.23 to 28.13%. Illite ranges between 6.26 and 17.47% with a mean of 10.79%. The palygorskite levels are less variable, with values ranging from 6.09 to 14.18% with an average of 9.46% (Fig. 7).

Table 2: Relative percentages of clay minerals determined in the sabkha deposits

Sample No.	Smectite	Chlorite	Kaolinite	Palygorskite	Illite
1	34.52	28.76	19.73	7.64	9.35
2	43.64	12.13	28.13	8.08	8.02
3	47.08	20.14	20.42	6.10	6.26
4	32.19	29.18	15.23	10.78	12.62
5	32.48	22.96	18.52	14.18	11.86
6	31.83	21.11	16.25	13.34	17.47
7	40.37	20.08	23.54	6.09	9.92
Max.	47.08	29.18	28.13	14.18	17.47
Min.	31.83	12.13	15.23	6.09	6.26
Aver.	37.44	22.05	20.26	9.46	10.79

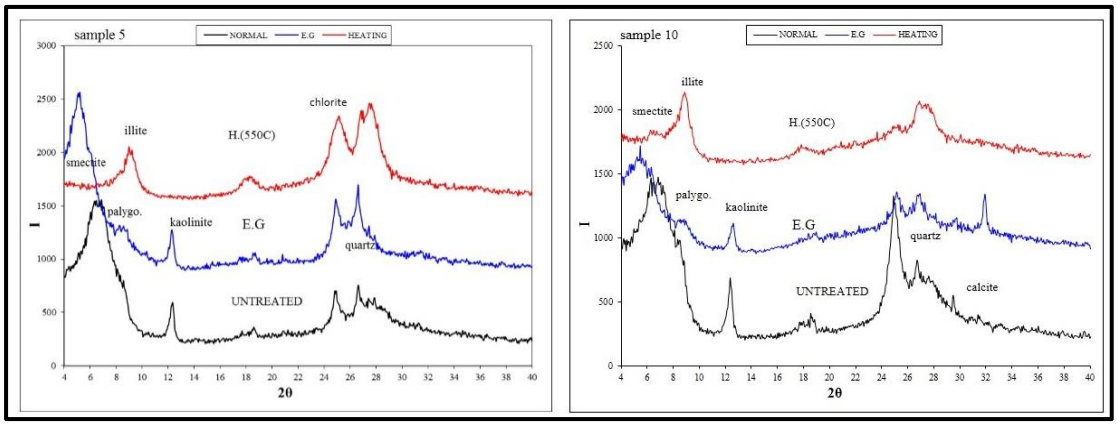

Fig. 6. X-ray diffractograms of the representative clay fraction of the sabkha sediments

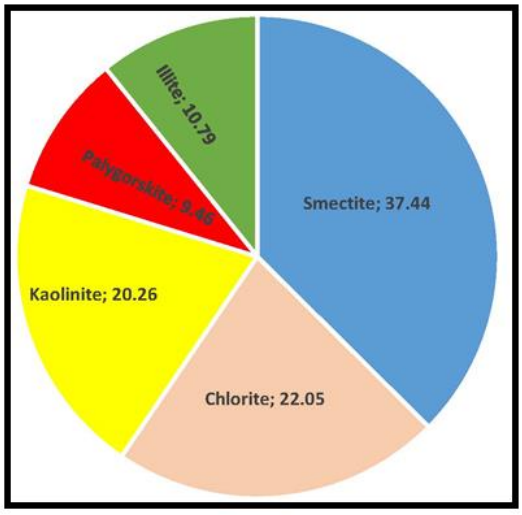

Fig. 7. The clay minerals percentage in the sabkha sediments

Table (3) shows the chemical analyses of some major elements (oxides) as well as trace elements determined in the studied by the extraction method.

Table 3: Concentrations of the extracted major oxides (%) and the trace elements (ppm) in the studied sediments.

Elements	The Current Study											A	B	C	D
	1	2	3	4	5	6	7	8	9	10	Mean				
Ca %	10.20	6.40	7.50	8.30	4.90	1.14	2.95	1.78	2.13	2.02	4.73		12.13	3.51	7.9
Na %	1.21	1.18	1.41	0.92	1.29	0.95	0.43	1.63	0.17	0.28	0.95				
K %	0.68	0.53	1.21	0.42	0.53	1.72	1.62	2.18	1.46	1.35	1.17				
Fe %	0.71	2.21	0.34	0.42	2.28	0.44	0.66	0.53	0.45	0.44	0.85		0.39	7.67	1.74
Mg %	0.74	1.34	1.83	3.12	1.21	0.55	0.82	0.37	0.62	0.72	1.13		0.053	1.65	1.9
Mn	0.29	0.14	0.54	0.25	0.51	0.49	0.67	0.35	0.44	0.47	0.41			0.15	0.31
Cu	8.08	14.35	6.98	3.09	12.54	2.51	1.64	2.15	1.34	2.65	5.53	2.1	7	28.78	14
Zn	43.61	57.23	21.28	28.12	48.49	16.45	23.12	26.21	20.86	24.53	30.99	4.46	20		38
Cd	0.31	0.59	1.38	0.38	1.38	0.54	0.58	0.43	0.65	0.62	0.69				
Ni	18.76	21.25	1.02	18.35	16.48	0.88	1.07	0.28	1.25	1.58	8.09				22
Pb	8.57	1.38	0.34	10.18	3.25	0.08	0.71	1.89	0.18	0.08	2.67		4		
Co	1.14	2.85	2.38	8.12	0.52	1.57	1.61	3.84	4.12	3.13	2.93	1.8			21
TCO3 %	18.51	17.15	41.70	32.84	16.39	15.65	8.96	9.57	8.96	15.79	18.55				
OM %	0.87	0.73	0.87	0.57	0.71	0.56	0.76	0.67	0.36	0.65	0.68				

A: Southern of Sinai, Red Sea (Gavish, 1980).

B: Jeddah, Red Sea Coast (Gheith and Basaham, 2013).

C: Al qahmah Sabkha, SE Red Sea, Saudi Arabia (Nabhan and Yang, 2018).

D: Al‑Lith Coastal Sediments, Red Sea Saudi Arabia (Bantan et al., 2020).

Table 4: Correlation coefficients matrix between the geochemical variables for the studied sabkha sediments

	Ca %	Na %	K %	Fe %	Mg %	Mn	Cu	Zn	Cd	Ni	Pb	Co	Carbonate %	Organic Matter %	Mud
Ca %	1.00														
Na %	0.41	1.00													
K %	-0.77	-0.13	1.00												
Fe %	0.17	0.30	-0.55	1.00											
Mg %	0.62	0.15	-0.65	0.03	1.00										
Mn	-0.46	-0.33	0.48	0.29	-0.30	1.00									
Cu	0.52	0.51	-0.70	0.88	0.18	-0.41	1.00								
Zn	0.51	0.39	-0.71	0.88	0.12	-0.58	0.90	1.00							
Cd	0.04	0.23	-0.17	0.35	0.15	0.47	0.42	0.08	1.00						
Ni	0.74	0.32	-0.90	0.64	0.49	-0.69	0.74	0.86	-0.10	1.00					
Pb	0.74	0.26	-0.62	0.00	0.58	-0.51	0.14	0.33	-0.36	0.71	1.00				
Co	0.12	-0.15	-0.13	-0.36	0.64	-0.45	-0.38	-0.24	-0.39	0.11	0.42	1.00			
Carbonate %	0.65	0.36	-0.44	-0.17	0.78	-0.11	0.21	-0.05	0.40	0.21	0.33	0.30	1.00		
Organic Matter %	0.56	0.56	-0.23	0.21	0.07	0.06	0.49	0.39	0.26	0.25	0.17	-0.48	0.37	1.00	
Mud	-0.25	0.09	0.54	-0.38	-0.10	0.67	-0.26	-0.56	0.45	-0.70	-0.60	-0.28	0.31	0.33	1.00

Discussion

Bulk Mineralogy of the Sabkha Sediments

In general, the mineralogy of the coastal sabkha sediments could explain the mode of formation, the diagenetic process, and the kind of the source rocks from which the different detrital components were derived.

The occurrence of gypsum crust in the studied sabkha is due to the upwards seepage of brine by capillary action and its evaporation at the surface. This mechanism is similar to what is happening in Abu Dhabi (Watson, 1979; Wilson et al., 2013). This suggests that the sulfates had been precipitated secondly after the carbonate and followed by halite indicating their possible development by sedimentation from brines migrating upward by the pumping mechanism of evaporation as recommended by means of Hsü and Schneider (1973).

The carbonate minerals in the studied area could belong to precipitation after the takeover of seawater to the sabkha during high tides, or it can be considered a contemporaneous dolomitization process, which is encouraged by the availability of calcium and magnesium ions, as well as the high temperatures within a supra-saline environment.

The occurrence of calcite near the water table in the studied area is most probably related to its evaporitic precipitation origin. The association of calcite with dolomite and/or aragonite (Table 1) is most probably attributed to the diagenetic alteration of the carbonate minerals of the bioclasts and shells, which were seen in these components in the sabkha sediments simple proportion. The formation of evaporite minerals and their distribution are controlled by the composition and the direction of the groundwater (Kendall, 1992).

The major amount of the carbonate could be of direct precipitation, and a minor amount is transported from seawater. Meaning the carbonate minerals resulted from direct chemical precipitation and part of that is related to the existence of shells and bioclasts derived from the coastal area.

The presence of the detrital minerals reflects the partly siliciclastic nature of the studied sabkha. This is due to the transportation of the fine detrital influx by windblown from the southeast.

In general, there is a notable concentration in the detrital constituents that controlled significant differences in the percentage of minerals, where the detrital sediments increase eastward away from the coastline. The presence of quartz and plagioclase feldspar could prove the derivation from the land either by aeolian transportation or brought through ancient wadis to the marine environment. The dominance of plagioclase feldspar over K-feldspar can be attributed to the volcanic origin from the eastern side, which is represented by an abundance of igneous rocks (El-Younsy et al., 2017).

Clay Mineralogy of the Sabkha Sediments

Clay minerals are essential components in the marine sediments along with chemical element concentrations and content assemblages, which are useful tools to find out the provenance, weathering intensity, and transport patterns (Kumar et al., 2011; Li et al., 2017; Zhang et al., 2020; Huang et al., 2021; Al-Amery and Al-Saad, 2022) . The clay mineral assemblage identified in the sabkha of the studied area (Table 2) is, smectite, chlorite, kaolinite,

illite, and palygorskite arranged in decreasing order of abundance (Fig. 6 and 7). The results reveal that smectite is the most abundant in the sabkha samples. This could be linked to the chemical weathering of volcanic rocks (Chamley, 1989; Perri et al., 2012).

It is possible that the availability of volcanic rocks on the surface and near the study area also, based on all the hypotheses put forward by researchers on this point, it is easy to conclude that the flocculation processes lead to an increase in the percentage of smectite and illite in the region. The diagenetic process modifies the volcanic glass, which results in the formation of the smectite lattice (Andreozzi et al., 1997; Pehlivanoglou et al., 2000; Fesneau et al., 2009; Perri et al., 2012). Hence, the alteration of pyroclastic and/or volcaniclastic rocks is probably responsible for the abundance of smectite. Typically, pyroclastic mafic rocks and tuffaceous deposits, are the source of smectite (Pettijohn, 1975), where, the eastern Red Sea mountainous escarpment is made up of basic (basalt and andesite), acidic (dacite and rhyolite) volcanic rocks, and granitic rocks. Consequently, it could be concluded that the increase in the percentage of smectite is due to the clastic origin and its derivation from the basic volcanic rocks, which agrees with the conclusion of El-Younsy et al.(2017).

The presence of chlorite can be attributed to the weathering products of metamorphic and volcanic rocks (Diekmann et al., 2000; Hillenbrand et al., 2003; Zhang et al., 2020). Accordingly, the mineral is primarily associated with the weathering products of igneous and metamorphic rocks and the contribution of detrital fine-grained sediments from these provenances to the studied area in the sabkha sediment samples.

Kaolinite mineral probably results from the intense chemical weathering of feldspar minerals in humid climates of tropical to subtropical with appropriate alkalis leaching (Grim, 1968; Keller, 1970; Perri and Ohta, 2014; Nayak et al., 2021). As a result of the intense chemical weathering of acidic igneous rocks under tropical to subtropical climate conditions in the source area, the relative content of the kaolinite raises the belief that its source is from the east of the study area (Pardo et al., 1999; Zhang et al., 2020; Huang et al., 2021).

The illite mineral is very similar to chlorite, which is an extract of the physical weathering of igneous rocks, especially acidic igneous rocks which are comparatively resistant to transportation agents (Ehrmann et al., 2007; Zhang et al., 2020). In this area, the illite could frequently accumulate in saline and semiarid hot environment, where the groundwater levels vary such as in the sabkha and wadi deposits in Saudi Arabia (Jado and Zötl, 1984).

It is known that palygorskite is the product of the alteration of hydrothermal solutions of pyroxene and amphibole. In most cases, palygorskite is an authigenic mineral in the lagoon as a result of the interaction of fresh water with marine water (Bouza et al., 2007). Palygorskite may be precipitated in situ from highly saline groundwater as is in coastal sabkhas or it could form in situ as a result of the interaction of magnesium-rich groundwater with other clay minerals in shallow coastal lagoon environments (Weaver, 1984; Cavalcante et al., 2011; Galan and Pozo, 2011). Therefore, the high percentage of palygorskite in the studied sabkha sediments could be related to authigenic origin. This is what Albadran and Hassan (2003) indicated about the authigenic formation of a palygorskite mineral within Khor Al -Zubair area, which is somewhat like the current study area.

Geochemistry of the Sabkha Sediments

The provenance and weathering could play a major role in the geochemistry of clastic sediments. Thus, the geochemical analysis of the sediment enables deciphering the geological evolution of a sedimentary unit or basin province from its source region (Bantan et al., 2020; Rahman et al., 2020; Papadopoulos et al., 2021; Tao et al., 2021; Mohanty et al., 2023) .

The carbonate content in the studied samples indicates a relatively low percentage in the sabkha sediments except for one sample which was 41.70% near the beach, which could be the direct precipitation from seawater (Table 3).

The total organic matter content in the studied samples indicates a relatively low percentage in the sabkha sediments. It ranges from 0.36 to 0.87% (Table 3), which can be attributed to some extent to the biological activities in the region especially in areas covered with vegetation. This may be linked to the rapid oxidation of organic carbon in these sediments. It could also be attributed to the difficult environmental conditions represented by the increase in salinity, in which the living of some organisms is difficult.

The variation in concentrations of elements is mentioned in (Table 3). The chemical analysis by extraction method does not give identical results with the mineral analysis that appears through X-ray diffraction analysis because of what was mentioned in the method of work that the analysis by extraction does not represent the total amount of elements present in the minerals, which sometimes gives the impression that the analysis method is inaccurate. However, despite this, the research is able to provide fairly good relationships. Pearson correlation with a significance level (P) less than 0.05, is applied for the relationships between geochemical variables. Calcium concentration exhibits a positive correlation (0.65) with carbonates (Table 4). This means that the calcium enrichment in the sediments could be associated with the supply of biogenic carbonates in the sabkha sediments. It also shows a positive correlation with Pb, Ni, Zn, and Cu (Table 4). The relatively low percentage of carbonate minerals and Ca in the sabkha sediments is probably due to the removal of calcium through gypsum precipitation (Patterson and Kinsman, 1982; Rosenberg et al., 2018).

A positive correlation appears between magnesium with calcium and carbonates (r =0.62 and 0.78 respectively), which means that magnesium is derived from the carbonate minerals (Mohammed et al., 2021). It also has a positive correlation with Co, Pb, and Ni (Table 4).

The positive correlations of manganese with iron, and mud and a negative relationship with the carbonate content can indicate the terrigenous origin arrived by wadis and wind. Other studies (Bantan et al., 2020; Nabhan and Yang, 2018), confirmed the similar observations.

The spatial distribution of the gypsum, halite, carbonate, Ca, Mg and Na in the sediments of Yakhtul sabkha (Fig. 8) indicates that gypsum content is observed to be the highest in the mid of the sabkha, and decreases into two directions; to the south and northeast side of the sabkha (Fig. 8a). Halite content is noticed in the middle of sabkha with increasing to northwest side of the sabkha and decreases to the east side of the sabkha (Fig. 8b). Carbonate increases in the western side of the sabkha and decreases to the east side of the sabkha (Fig. 8c). The Ca concentration is low at the northern and southern parts of the sabkha and increases in the western side of the sabkha (Fig. 8d). The Mg concentration increases in the western part of the sabkha and decreases in the eastern part of the sabkha (Fig. 8e). The Na increases in the mid of

the sabkha, and decreases to the northern side of the sabkha (Fig. 8f). Ca and Mg are noticed in limited distribution due to the presence of chemically precipitated of some calcite and dolomite in the analyzed sabkha deposits, and this could be related to the weak delivery of sea water to the studied sabkha. All these data indicate that most of the elements come from the eastern side and are concentrated in the sabkha, in addition to the elements that were deposited in the place due to high evaporation.

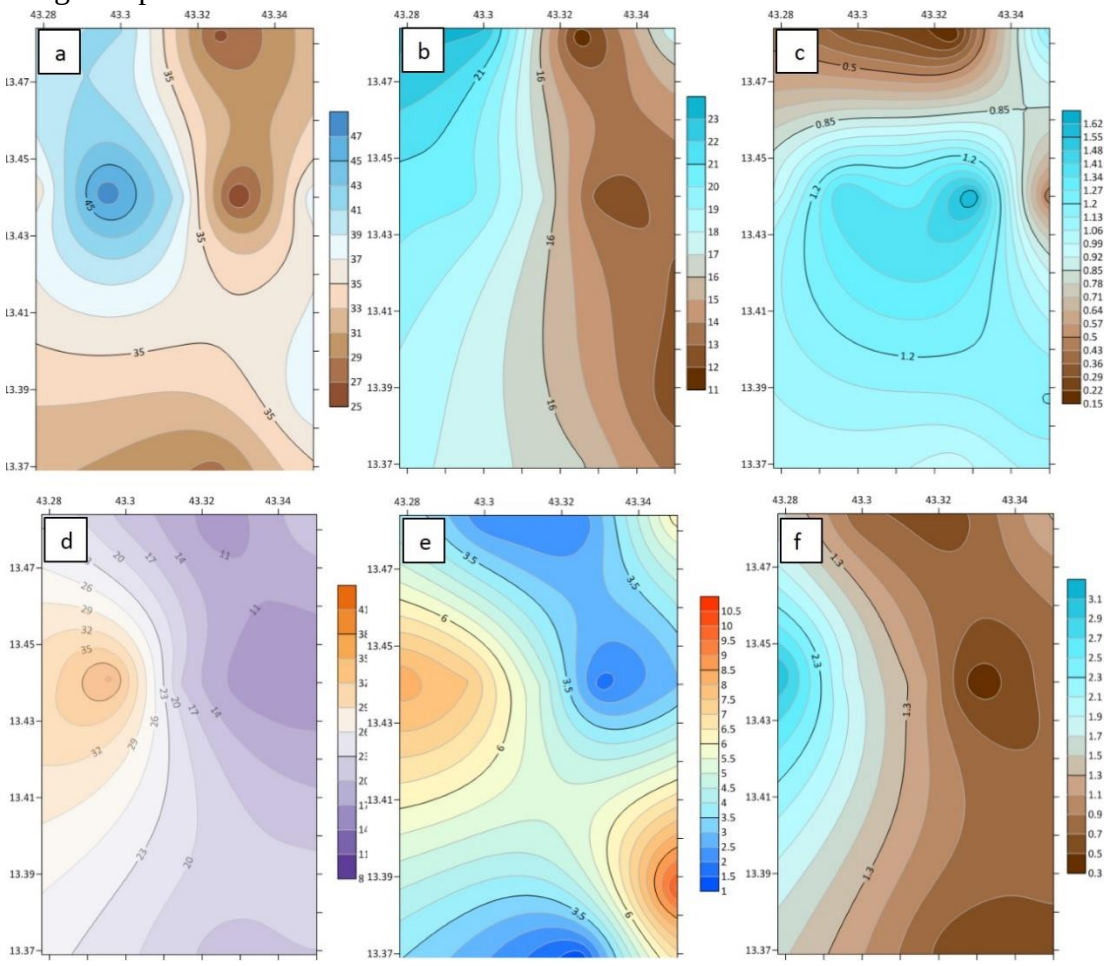

Fig. 8. Spatial distributions of the gypsum (a), halite (b), carbonate(c), Ca (d), Mg (e) and Na (f) in the sediments of Yakhtul sabkha

Comparing the results of this study with the results of the previous studies for some near Red Sea sabkhas indicates that the average of major and trace element contents in the studied sabkha sediments compared with other sabkha sediments along the Red Sea are given in Table (3). This comparison reveals that the Red Sea sabkha contains a smaller percentage of calcium than that of the southern Jeddah sabkha and Al‑Lith sabkha. The iron content is relatively lower than that recorded in Al Qahmah sabkha and Al‑Lith sabkha. This trend is due to the presence of low content of detrital minerals in Red Sea sabkha deposits. The magnesium content is relatively lower than that recorded in Al Qahmah sabkha and Al-Lith sabkha, which may be attributed to the presence of dolomite with low proportion. Most of the concentration of trace elements in the studied sabkha sediments are lower than in recorded other Red Sea sabkha. There is a possibility that the method of analysis by extraction is one of the factors that led to the difference in the results.

The results mentioned above illustrate that the distribution of the major elements and trace elements in the studied sabkha sediments indicate that most of these elements are mainly derived from the source rocks outcropping to the east of the study area.

Conclusions

The Current study has revealed the following:

1- The evaporite sabkha in the Red Sea is induced by the evaporation of lagoonal water as well as underground water seepages as continental influx.

2- The evaporitic minerals in the studied sabkha include gypsum, halite, and anhydrite. Carbonate minerals are represented by calcite, aragonite, and dolomite, whereas quartz, plagioclase, and K-feldspar represent non-evaporite minerals. Halite encrustations mostly reflect well-developed sabkhization.

3- The appearance of some aggregates of clay minerals, and non-evaporite minerals can be considered as clastic coming from the igneous and metamorphic source rocks to the east of the study area.

Acknowledgments

The authors are very grateful to the Editor-in-Chief of INJES journal and the reviewers for their constructive comments to improve the manuscript.

Conflict of Interest

The authors declare that there are no conflicts of interest regarding the publication of this manuscript.

References

Al-Amery, A.N. and Al-Saad, H.A., 2022. Mineralogical Variation of the Banks of Shatt Al-Arab and Shatt Al-Basrah River Sediments in Southern Iraq. Iraqi Geol J55 (1A), 116–127. http://doi.org/10.46717/igj.55.1A.9Ms-2022-01-28

Albadran, B.N. and Hassan, W.F., 2003. Clay minerals distribution of supratidal regions, south of Iraq. Mar. Mesopotamica 18(1), 25–33.

Albadran, B.N. and Al-Kaaby, L.F., 2021. Microbial and Physical Sedimentary Structures in the Tidal Flats of Khor Al-Zubair, NW of Arabian Gulf, in: Jawad, L. A. (Ed.), The Arabian Seas: Biodiversity, Environmental Challenges and Conservation Measures. pp. 277–295. https://doi.org/10.1007/978-3-030-51506-5_12

Andreozzi, M., Dinelli, E. and Tateo, F., 1997. Geochemical and mineralogical criteria for the identification of ash layers in the stratigraphic framework of a foredeep; the Early Miocene Mt. Cervarola Sandstones, northern Italy. Chem Geol 137, 23–39. https://doi.org/10.1016/S0009-2541(96)00148-9

Aref, M.A.M., Basyoni, M.H. and Bachmann, G.H., 2014. Microbial and physical sedimentary structures in modern evaporitic coastal environments of Saudi Arabia and Egypt. Facies 60, 371–388. https://doi.org/10.1007/s10347-013-0379-8

Attia, O.E.A., 2013. Sedimentological characteristics and geochemical evolution of Nabq sabkha, Gulf of Aqaba, Sinai, Egypt. Arab J Geosci 6, 2045–2059. https://doi.org/10.1007/s12517-011-0499-9

Bantan, R.A., Khawfany, A.A., Basaham, A.S. and Gheith, A.M., 2020. Geochemical Characterization of Al-Lith Coastal Sediments, Red Sea, Saudi Arabia. Arab J Sci Eng 45, 291–306. https://doi.org/10.1007/s13369-019-04161-6

Bouza, P.J., Simón, M., Aguilar, J., Valle, H. and Rostagno, M., 2007. Fibrous-clay mineral formation and soil evolution in Aridisols of northeastern Patagonia, Argentina. Geoderma 139, 38–50. https://doi.org/10.1016/j.geoderma.2007.01.001

Carver, R.E., 1971. Procedures in Sedimentary Petrology, New York, Wiley Interscience, 653 p.

Cavalcante, F., Belviso, C., Bentivenga, M., Fiore, S. and Prosser, G., 2011. Occurrence of palygorskite and sepiolite in upper Paleocene – middle Eocene marine deep sediments of the Lagonegro Basin (Southern Apennines — Italy): Paleoenvironmental and provenance inferences. Sediment Geol 233, 42–52. https://doi.org/10.1016/j.sedgeo.2010.10.007

Chamley, H., 1989. Clay Sedimentology. Springer-Verlag Berlin Heidelberg, 626 p. https://doi.org/10.1007/978-3-642-85916-8

Chao, G.Y., 1969. 2θ (Cu) table for common minerals: Geological paper 69-2. Carleton University, Ottawa, Canada, Carleton University, Ottawa, Canada.

Chen, P.Y., 1977. Table of key lines on X-ray powder Diffraction patterns of Minerals in clays and associated rocks. Department of Natural Resources Geological survey paper 21.

Cohen, Y., Krumbein, W. and Shilo, M., 1977. Solar Lake (Sinai) 2 distribution of photosynthetic microorganisms and primary production. Limnol Ocean 22, 609–620. https://doi.org/10.4319/LO.1977.22.4.0609

Dean, W.E., 1974. Determination of carbonate and organic matter in calcareous sediments and sedimentary rocks by loss on ignition; comparison with other methods. J Sediment Res 44, 242–248. https://doi.org/10.1306/74D729D2-2B21-11D7-8648000102C1865D

Diekmann, B., Kuhn, G., Rachold, V., Abelmann, A., Brathauer, U., Fütterer, D.K., Gersonde, R. and Grobe, H., 2000. Terrigenous sediment supply in the Scotia Sea (Southern Ocean): response to Late Quaternary ice dynamics in Patagonia and on the Antarctic Peninsula. Palaeogeogr Palaeoclimatol Palaeoecol 162, 357–387. https://doi.org/10.1016/S0031-0182(00)00138-3

Edward, A.J., Head, S.M., 1987. Red Sea. Key environments Series. Pergamon Press, Oxford, 441 p.

Ehrmann, W., Schmiedl, G., Hamann, Y., Kuhnt, T., Hemleben, C. and Siebel, W., 2007. Clay minerals in late glacial and Holocene sediments of the northern and southern Aegean Sea. Palaeogeogr Palaeoclimatol Palaeoecol 249, 36–57. https://doi.org/10.1016/j.palaeo.2007.01.004

El-Younsy, A.R., Essa, M.A. and Wasel, S.O., 2017. Sedimentological and geoenvironmental evaluation of the coastal area between Al-Khowkhah and Al-Mokha, southeastern Red Sea, Yemen. Environ Earth Sci 76, 1–22. https://doi.org/10.1007/s12665-016-6355-1

Fesneau, C., Deconinck, J.-F., Pellenard, P. and Reboulet, S., 2009. Evidence of aerial volcanic activity during the Valanginian along the northern Tethys margin. Cretac Res 30, 533–539. http://dx.doi.org/10.1016/j.cretres.2008.09.004

Galan, E. and Pozo, M., 2011. Palygorskite and sepiolite deposits in continental environments. Description, genetic patterns, and sedimentary settings, in: Developments in Palygorskite-Sepiolite Research. A New Outlook on These Nanomaterials. In: Galan E and Singer E (Eds.), Developments in Clay Science. Elsevier, Amsterdam, 3, pp. 125–173. https://doi.org/10.1016/B978-0-444-53607-5.00006-2

Galehouse, J.S., 1971. Sedimentation analysis. Proceed Sediment Petrol 69–94.

Gavish, E., 1980. Recent sabkhas marginal to the southern coasts of Sinai, Red Sea, in: In: Nissenbaum A (Ed) Hypersaline Brines and Evaporitic Environments. Developments in Sedimentology. Elsevier, Amsterdam, 28, pp. 233–251.

Gerdes, G. and Krumbein, W., 1987. Biolaminated deposits. Lecture notes in Earth Science. Springer, Berlin, 9, 190 P.

Gheith, A.M. and Basaham, A.S., 2013. Mineralogical and Chemical Significances of Modern Marine Sabkha, Developed in the Southern Corniche Beach of Jeddah, Red Sea Coast. Dev Appl Ocean Eng Vol 2(1), 8–14.

Grim, R.E., 1968. Clay Mineralogy, International series in the Earth and planetary sciences, 2nd.ed. McGraw Hill, New York, 596 P.

Hillenbrand, C., Grobe, H., Diekmann, B., Kuhn, G. and Fütterer, D.K., 2003. Distribution of clay minerals and proxies for productivity in surface sediments of the Bellingshausen and Amundsen seas (West Antarctica) - Relation to modern environmental conditions. Mar Geol 193, 253–271. https://doi.org/10.1016/S0025-3227(02)00659-X

Hsü, K.J. and Schneider, J., 1973. Progress report on dolomitization—hydrology of Abu Dhabi sabkhas, Arabian Gulf, in: The Persian Gulf: Holocene Carbonate Sedimentation and Diagenesis in a Shallow Epicontinental Sea. Springer, pp. 409–422.

Huang, J., Jiao, W., Liu, J., Wan, S., Xiong, Z., Zhang, J., Yang, Z., Li, A. and Li, T., 2021. Sediment distribution and dispersal in the southern South China Sea: Evidence from clay minerals and magnetic properties. Mar Geol 439, 106560. https://doi.org/10.1016/j.margeo.2021.106560

Jado, A.R. and Zötl, J., 1984. Quaternary period in Saudi Arabia. Springer-Verlag Wien, 354 P.

Keller, W.D., 1970. Environmental aspects of clay minerals. J Sediment Res 40, 788–813.

Kendall, A., 1992. Evaporites, In: Walker RG and James NP (Ed) Facies Models- Response to Sea Level Change. Geoscience Canada, pp. 39–58. https://doi.org/10.1017/S0016756800020331

Kendall, C.S.C. and Warren, J., 1987. A review of the origin and setting of tepees and their associated fabrics. Sedimentology 34, 1007–1027. https://doi.org/10.1111/J.1365-3091.1987.TB00590.X

Kinsman, D.J.J., 1969. Modes of formation, sedimentary associations, and diagnostic features of shallow-water and supratidal evaporites. Am Assoc Pet Geol Bull 53, 830–840. https://doi.org/10.1306/5D25C801-16C1-11D7-8645000102C1865D

Kumar, A., Khan, M.A. and Muqtadir, A., 2011. Distribution of Mangroves along the Red Sea Coast of the Arabian Peninsula: Part-3: Coast of Yemen. Earth Sci India 4, 29–38. https://doi.org/10.1007/s12145-010-0061-4

Lakhdar, R., Soussi, M. and Talbi, R., 2021. Modern and Holocene microbial mats and associated microbially induced sedimentary structures (MISS) on the southeastern coast of Tunisia (Mediterranean Sea). Quat Res 100, 77–97. https://doi.org/doi.org/10.1017/qua.2020.91

Li, J., Liu, S., Shi, X., Feng, X., Fang, X., Cao, P., Sun, X. and Khokiattiwong, S., 2017. Distributions of clay minerals in surface sediments of the middle Bay of Bengal: source and transport pattern. Cont Shelf Res 145, 59–67. https://doi.org/10.1016/j.csr.2017.06.017

Loring, H.D. and Rantala, R., 1992. Manual for the Geochemical Analyses of Marine Sediments and Suspended Particulate Matter. Earth-Science Review, 32, 235-283. http://dx.doi.org/10.1016/0012-8252(92)90001-A

Manaa, A.A. and Aref, M.A., 2022. Microbial mats and evaporite facies variation in a supralittoral, ephemeral lake, Red Sea coast, Saudi Arabia. Facies 68:3, 1–21. https://doi.org/doi.org/10.1007/s10347-021-00641-0

Mohammed, A.A., Anan, T.I. and Gheith, A.M., 2021. Distribution and Significances of the Major Oxides in Recent Coastal Sabkha Sediments of the Al-Dafna Plateau, Northeast Tobruk, Libya. Sci J Fac Sci Univ 1(2), 12–19. https://doi.org/doi.org/10.37375/sjfssu.v1i2.82

Mohanty, S., Adikaram, M. and Sengupta, D., 2023. Geochemical, mineralogical, and textural nature of beach placers, north-east Sri Lanka: Implications for provenance and potential resource. Int J Sediment Res 38, 279–293. https://doi.org/10.1016/j.ijsrc.2022.09.004

Nabhan, A.I. and Yang, W., 2018. Modern sedimentary facies, depositional environments, and major controlling processes on an arid siliciclastic coast, Al qahmah , SE Red Sea , Saudi Arabia. J African Earth Sci 140, 9–28. https://doi.org/10.1016/j.jafrearsci.2017.12.014

Nayak, K., Lin, A.T.-S., Huang, K.-F., Liu, Z., Babonneau, N., Ratzov, G., Pillutla, R.K., Das, P. and Hsu, S.-K., 2021. Clay-mineral distribution in recent deep-sea sediments around Taiwan: Implications for sediment dispersal processes. Tectonophysics 814, 228974. https://doi.org/10.1016/j.tecto.2021.228974

Noffke, N., 2010. Geobiology Microbial Mats in Sandy Deposits from the Archean Era to Today. Springer, Heidelberg-Dordrecht-London-New York 200 P. ISBN 978-3-642-12771-7. http://dx.doi.org/10.1007/978-3-642-12772-4

Papadopoulos, A., Lazaridis, S., Kipourou-Panagiotou, A Kantiranis, N., Koroneos, A. and Almpanakis, K., 2021. Mineralogy, Geochemistry and Provenance of Coastal Sands from Greece: New Insights on the REE Content of Black Coastal Sands from Aggelochori Area, N.-Greece. Minerals 11, 1–13. http://doi.org/10.3390/min11070693

Pardo, A., Adatte, T., Keller, G. and Oberhänsli, H., 1999. Paleoenvironmental changes across the Cretaceous–Tertiary boundary at Koshak, Kazakhstan, based on planktic foraminifera and clay mineralogy. Palaeogeogr Palaeoclimatol Palaeoecol 154, 247–273. https://doi.org/10.1016/S0031-0182(99)00114-5

Patterson, R.J. and Kinsman, J., 1982. Formation of Diagenetic Dolomite in Coastal Sabkha Along Arabian (Persian) Gulf. Am Assoc Pet Geol Bull 66(1), 28–43.

Pehlivanoglou, K., Tsirambides, A. and Trontsios, G., 2000. Origin and distribution of clay minerals in the Alexandroupolis Gulf, Aegean Sea, Greece. Estuary Coast Shelf Sci 51, 61–73. https://doi.org/10.1006/ecss.1999.0620

Perri, F. and Ohta, T., 2014. Paleoclimatic conditions and paleoweathering processes on Mesozoic continental redbeds from Western-Central Mediterranean Alpine Chains. Palaeogeogr Palaeoclimatol Palaeoecol 395, 144–157. https://doi.org/10.1016/j.palaeo.2013.12.029

Perri, F., Critelli, S., Cavalcante, F., Mongelli, G., Dominici, R., Sonnino, M. and De Rosa, R., 2012. Provenance signatures for the Miocene volcaniclastic succession of the Tufiti di Tusa Formation, southern Apennines, Italy. Geol Mag 149, 423–442. http://dx.doi.org/10.1017/S001675681100094X

Pettijohn, F.J., 1975. Sedimentary rocks. Harper & Row New York, 628 P.

Purser, B.H., 1973. The Persian Gulf, Holocene Carbonate sedimentation and diagenesis in a shallow epicontinental sea. Springer-Verlag Berlin, 466 P.

Rahman, A., Das, S.C., Pownceby, M.I., Tardio, J., Alam, M.S. and Zaman, M.N., 2020. Geochemistry of Recent Brahmaputra River Sediments: Provenance, Tectonics, Source Area Weathering and Depositional Environment. Miner Artic 10,813, 1–30. https://doi.org/doi:10.3390/min10090813

Rosenberg, Y.O., Sade, Z. and Ganor, J., 2018. The precipitation of gypsum, celestine, and barite and coprecipitation of radium during seawater evaporation. Geochim Cosmochim Acta 233, 50–65. https://doi.org/10.1016/j.gca.2018.04.019

Rushdi, A., Abubaker, M. and Hebba, H., 1994. Marine Habitats of the Red Sea at Al Urj-Alsalif and Dhubab – Yokhtol areas, their ecology Environment and Management recommendations. Dept. of Oceanography, Faculty of Science, Sana'a University, Republic of Yemen, and UNDP, 117 P.

Tao, H., Hao, L., Li, S., Wu, T., Qin, Z. and Qiu, J., 2021. Geochemistry and Petrography of the Sediments from the Marginal Areas of Qinghai Lake, Northern Tibet Plateau, China: Implications for Weathering and Provenance. Front Earth Sci 9:725553. https://doi.org/10.3389/feart.2021.725553

Tucker, M.E., 1988. Techniques in Sedimentology. Blackwell Scientific Pub.396 P.

Wasel, S.O. and Al-Zubieri, A.G., 2023. Surface Texture of the Quartz Grains and Mineralogical Characteristics of Coastal Sabkha Sediments of South Hodeidah, Red Sea Coast, Yemen. under Prep.

Watson, A., 1979. Gypsum crusts in deserts. J Arid Environ 2, 3-20.

Weaver, C.E., 1984. Origin and geologic implications of the palygorskite deposits of SE United States, In: Singer A, Galan E (Eds) Developments in Sedimentology, Vol 37. Elsevier, Amsterdam, pp. 39–58.

Wilson, M.A., Shahid, S.A., Abdelfattah, M.A., Kelley, J.A. and Thomas, J.E., 2013. Anhydrite Formation on the Coastal Sabkha of Abu Dhabi, United Arab Emirates, In: Shahid, S. A., Taha, F. K., and Abdelfattah, M. A. (Eds.), Developments in Soil Classification, Land Use Planning and Policy Implications, pp. 175–201. https://doi.org/DOI 10.1007/978-94-007-5332-7_8

Zhang, M., Lu, H., Chen, Q., Bandara, G., Zhang, H., Luo, C. and Wu, N., 2020. Clay Mineralogy and Geochemistry of the Pockmarked Surface Sediments from the Southwestern Xisha Uplift, South China Sea: Implications for Weathering and Provenance. Geosciences 11, 8. https://doi.org/https://dx.doi.org/10.3390/geosciences11010008